

Research Article

# Flow Characteristics of Plane Jets Passing Over Two-Dimensional Flat Plates

K. Ishiwata<sup>1,\*</sup>  
K. Nishibe<sup>2</sup>  
K. Sato<sup>3</sup>

<sup>1</sup>Mechanical Engineering Program  
in the Graduate School of  
Engineering, Kogakuin University,  
Tokyo 192-0015, Japan

<sup>2</sup>Department of Mechanical  
Engineering, Tokyo City University,  
Tokyo 158-8557, Japan

<sup>3</sup>Department of Mechanical System  
Engineering, Kogakuin University,  
Tokyo 192-0015, Japan

Received 26 September 2023

Revised 30 November 2023

Accepted 8 December 2023

## Abstract:

*A simple model was proposed to consider situations in which jet flows pass over seats in high-speed trains and aircraft cabins. Efforts were made to understand the flow characteristics inside the cavity when jet flows pass over partition plates (2D flat plate arrays). Flow visualization experiments and numerical calculations were conducted, and various geometric conditions were investigated for typical flow patterns. It was demonstrated that the inflow rate into the cavity and size of the recirculation region formed inside the cavity depended on the offset ratio and length of the partition plate. In particular, the influence of the distance from the slot to the tip of the partition plate on the internal flow characteristics of the cavity was discussed.*

**Keywords:** Jet flow, Flat plates, Flow visualization, Velocity distribution

## 1. Introduction

Jet flows are widely utilized in various applications such as air conditioning and ventilation systems and have garnered increased attention since the outbreak of Covid-19, particularly in enclosed public spaces, such as high-speed trains, airplanes, buses, hospital waiting rooms, and schools [1]. Fundamental research on jet-flow technology has been actively pursued by many researchers [2-7], with the topics being diverse and discussed from various angles. It has been reported by ZHANG et al [8, 9] that directional control of jet flows can be achieved using the Coanda effect to generate secondary jets.

Despite their significant relevance to ventilation technologies in transportation vehicle cabins, systematic studies on the characteristics of jet flows over partition plates remain unexplored. Our focus extends beyond specific applications to examine the dynamics of jets moving through the upper sections of cavities created by partition plates. This includes scenarios such as in high-speed trains and aircraft, air conditioning systems in movie theaters and concert halls, and ventilation systems for hazardous substance removal in industrial settings.

In our study, we employ the smoke wire method for flow visualization, measure time-averaged velocity distributions using a hot-wire anemometer, and create velocity vector contour diagrams through numerical simulations. Our discussion centers on the behavior of jet flows, considering variables like the length of the partition plates, the offset ratio between the jet nozzle width and cavity depth, among other influential factors.

\* Corresponding author: K. Ishiwata  
E-mail address: am23008@ns.kogakuin.ac.jp



## 2. Experimental Setup and Numerical Calculation

Fig. 1 shows an overview of the experimental setup. Fig. 1(a) shows the top view in which the slot from which the jet flows are ejected is visible. The slot width is  $b_0 = 5.0 \times 10^{-3}$  m, and the continuous jet flows are ejected to the right in the figure. The test section area of the experimental setup was  $90b_0$  in the x-direction and  $200b_0$  in the y-direction. Fig. 2(b) shows the front view. The test section was sandwiched between two acrylic plates, and an approximately two-dimensional flow was realized near the central cross section. At this time, the slot height is  $h_0 = 100 \times 10^{-3}$  m, and the aspect ratio of the slot outlet is 20. The flow was generated using a blower and directed to the test section through a plenum tank and nozzle. The flow velocity was adjusted using an inverter and was controlled by the rotational speed of the blower. The inverter used is a Toshiba VFNC1-2007P, and the blower is a Showa Denki U75-2-R313. The entire experimental apparatus measures  $200b_0$  in x-direction and  $200b_0$  in y-direction. The velocity of the jet flow was measured at the slot outlet's central cross-section using a hot-wire anemometer, and this measured value was used as the representative velocity for our studies. For visualizing the flow, the smoke wire method was employed. Given the flow velocity range of 3.0 [m/s] in our experiments, preliminary trials were conducted to optimize the observation of visualization. Consequently, we chose to use the smoke wire method with fluid paraffin for its enhanced visibility. In this method, liquid paraffin is heated by an electric wire, producing white smoke that is then illuminated by a laser beam and captured with a digital camera. For the purposes of this study, the standard flow velocity was established at  $U_0 = 3.0$  m/s.

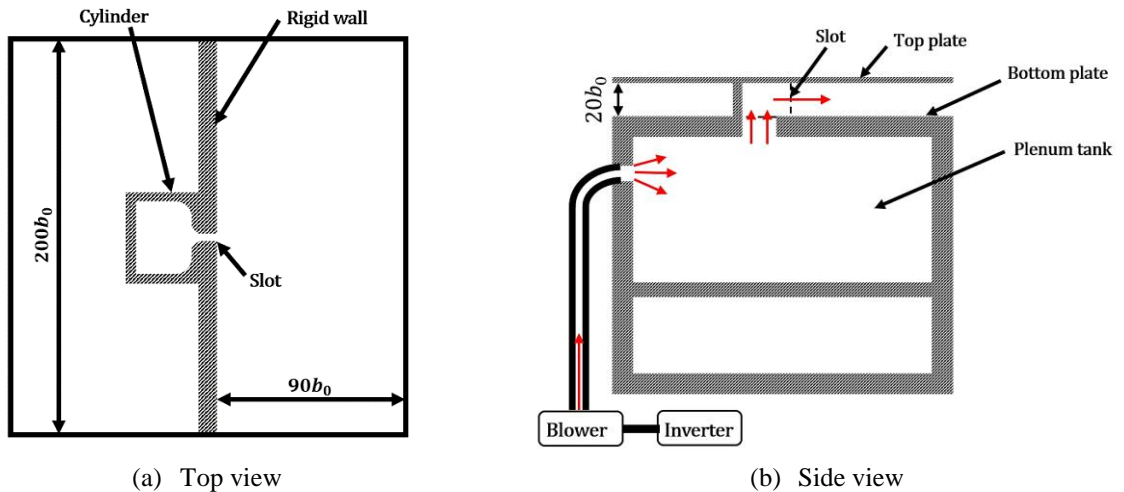


**Fig. 1.** Schematic diagram of experimental equipment

Fig. 2 shows the arrangement of the partition plates used in this experiment. Five partition plates were placed at equal intervals on the walls of an acrylic plate with a length of  $30b_0$ , to replicate the five cavities.

To effectively measure distance  $y_c$  from the center of the slot to the tip of the partition plate and to systematically assess its impact, the parameter representing the depth from the slot center is defined as the offset rate,  $H_s = h_s/b_0$ . Additionally, the dimensionless length of the partition plate is characterized as  $H_p = h_p/b_0$ . As  $H_s$  and  $H_p$  are parameters intrinsically linked to  $y_c$ , they were selected for use in this study.

Fig. 3 depicts the boundary conditions employed in the numerical analysis, which was conducted using ANSYS Fluent software. The flow field was modeled as a two-dimensional incompressible viscous flow, and an unsteady analysis was carried out. For the turbulence model, the k- $\epsilon$  model was chosen, and the mesh comprised approximately 50,000 elements.

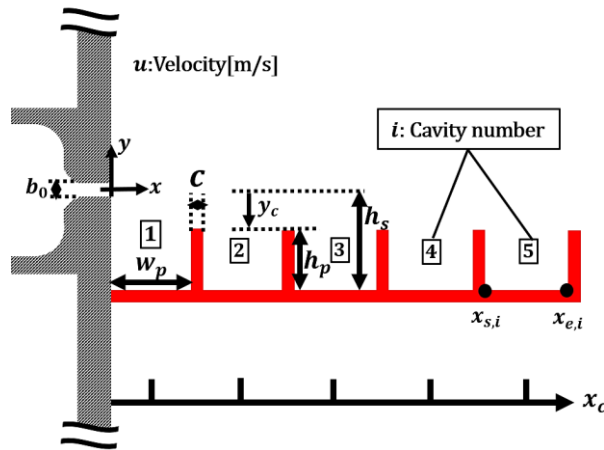


Fig. 2. Layout of partition plate

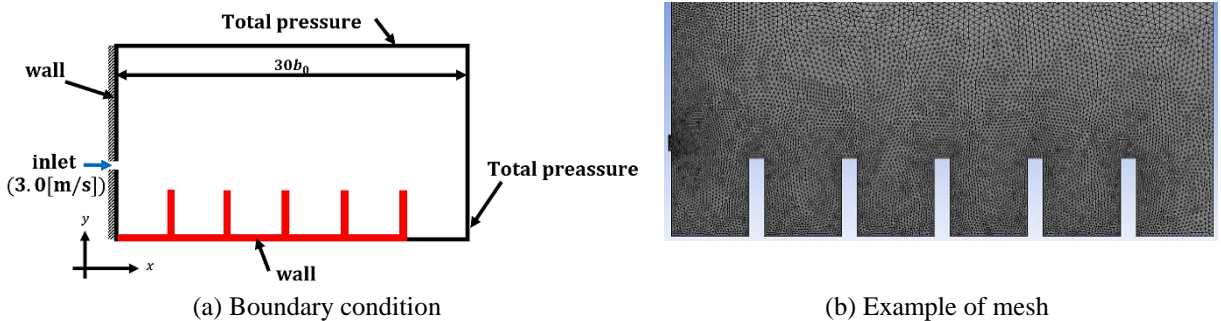
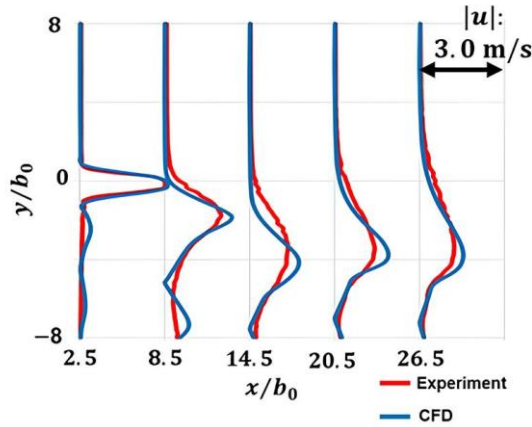


Fig. 3. Conditions for numerical analysis

In this study, preliminary calculations were performed to ascertain the ideal mesh count and select the most suitable turbulence model. We began by examining the mesh dependency of the flow field, using mesh sizes of approximately 8,000, 50,000, and 100,000. Time-averaged velocity distributions were analyzed under conditions of  $H_p = h_p/b_0 = 5$ ,  $H_s = h_s/b_0 = 10$ ,  $U_0 = 3.0$  [m/s], and  $b_0 = 5.0 \times 10^{-3}$  [m]. The accuracy of these simulations was gauged by comparing them with experimental data gathered using a hot wire anemometer. Based on these evaluations, this study primarily utilizes approximately 50,000 meshes, considering both the accuracy of the results and the computational expense involved.

In this section, the validation results of the turbulence model are presented. An unsteady two-dimensional flow was assumed, and the Unsteady Reynolds Averaged Navier-Stokes (URANS) equations were utilized as the governing equations. The selection of turbulence models was guided by their applicability to URANS, and preliminary calculations were performed to verify the  $k-\epsilon$  model,  $k-\omega$  model, and  $k-\omega$  SST model. In line with the verification of mesh dependency, comparisons were made between the numerical results of the time-averaged  $x$ -directional velocity (absolute value) distribution under conditions  $H_p = h_p/b_0 = 5$ ,  $H_s = h_s/b_0 = 10$ ,  $U_0 = 3.0$  [m/s] and  $b_0 = 5.0 \times 10^{-3}$  [m] and experimental data acquired using a hot-wire anemometer. The  $k-\epsilon$  model was adopted as the turbulence model for this study, as it was found to have the smallest overall error in each cross section, with the maximum error being approximately 6%.

Fig. 4 depicts a comparison of the experimental (red) and numerical (blue) velocity distributions, utilizing the  $k-\epsilon$  model with a 50,000 element mesh.



**Fig. 4.** Velocity distribution of  $k - \varepsilon$  model  
 (50,000 element mesh,  $H_p = h_p/b_0 = 5$ ,  $H_s = h_s/b_0 = 10$ ,  $U_0 = 3.0$  [m/s],  $b_0 = 5.0 \times 10^{-3}$  [m])

### 3. Results and Discussion

Figs. 5 and 6 show (a) flow visualization photographs and (b) numerical simulation results for jet flows generated with a slot width of  $b_0 = 5$  mm under the condition of velocity  $U_0 = 3.0$  m/s. In the flow visualization photographs (a), the trajectories of the jet flows obtained from the video observations are indicated by arrows. The numerical simulation results shown in (b) are represented by velocity contours and vector diagrams.

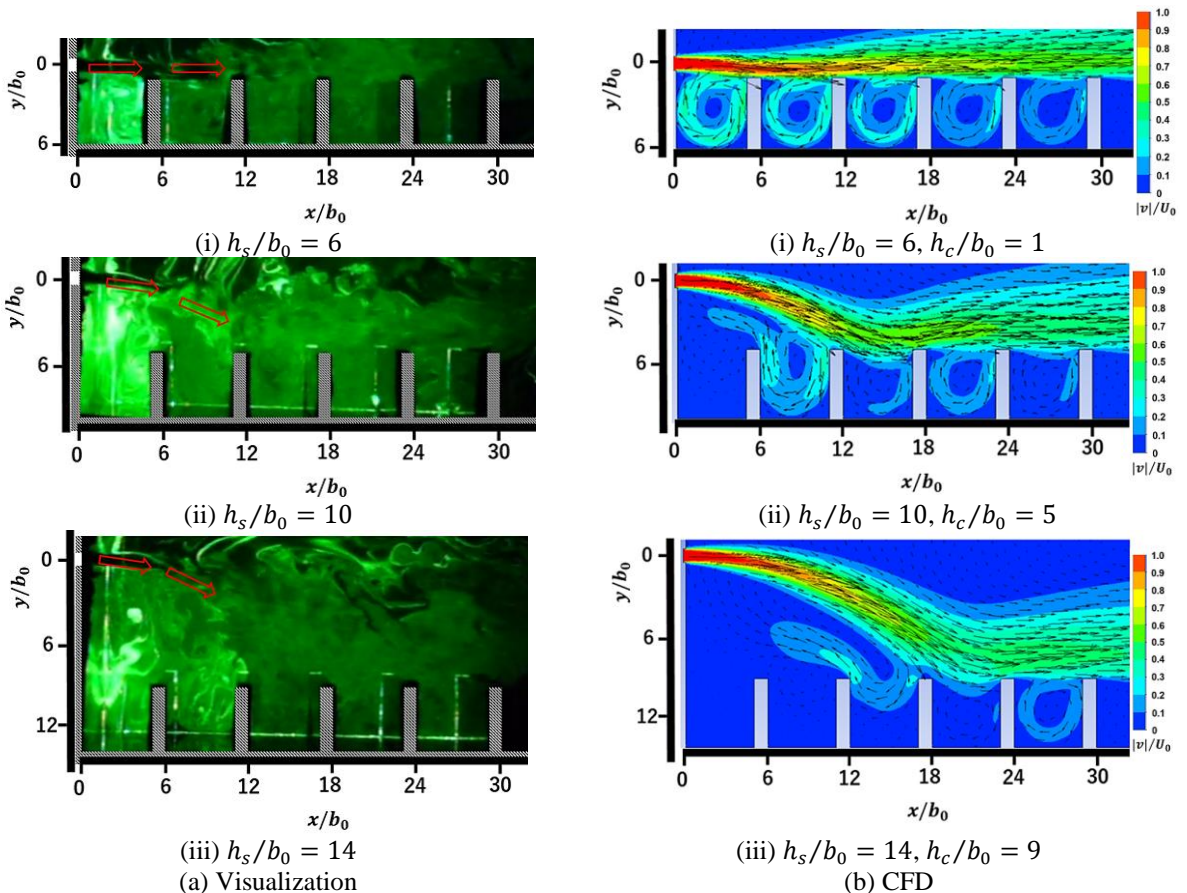


**Fig. 5.** Influence of offset ratio  
 ( $U_0 = 3.0$  m/s,  $H_p = h_p/b_0 = 5$ ,  $w = 25$  mm,  $b_0 = 5.0 \times 10^{-3}$  m)

Fig. 5 shows the influence of the offset ratio  $H$  on the distance from the slot to the bottom surface, while keeping the length of the partition plate  $h_p = 5b_0$  constant. The results for different values of  $h_s/b_0 = 6, 10, 14$  ( $y_c/b_0 = 1, 5, 9$ ) are presented in (i), (ii), and (iii), respectively. In the case of (i)  $h_s/b_0 = 6$ , where the relative distance from the slot to the bottom surface  $h_c/b_0$  is small, the jet flow behaves mostly straight despite the geometric boundary conditions being asymmetric for both the experiments and numerical calculations. Clockwise recirculation regions were observed inside all cavities, with the cavity at  $X_c = x_c/b_0 = 2.5$  closest to the jet outlet slot and receiving the largest inflow. In the cases of (ii)  $h_s/b_0 = 10$  and (iii)  $h_s/b_0 = 14$ , where the relative distances from the slot to the bottom surface or partition plate tip were large, the jet flow was deflected towards the partition plate side owing to the Coanda effect. The stagnation point resulting from the reattachment of the jet flow appeared on the second flat plate from the left for (ii)  $h_s/b_0 = 10$  and on the third flat plate from the left for (iii)  $h_s/b_0 = 14$ . Although the experimental and numerical results matched well, the flow visualization photographs in Fig. 5(a) are somewhat less clear. From the numerical simulation results in Fig. 5(b), it can be observed that the vorticity inside each cavity depends on  $h_s/b_0(y_c/b_0)$ , and that the cavity positions with the maximum vorticity differ among (i), (ii), and (iii).

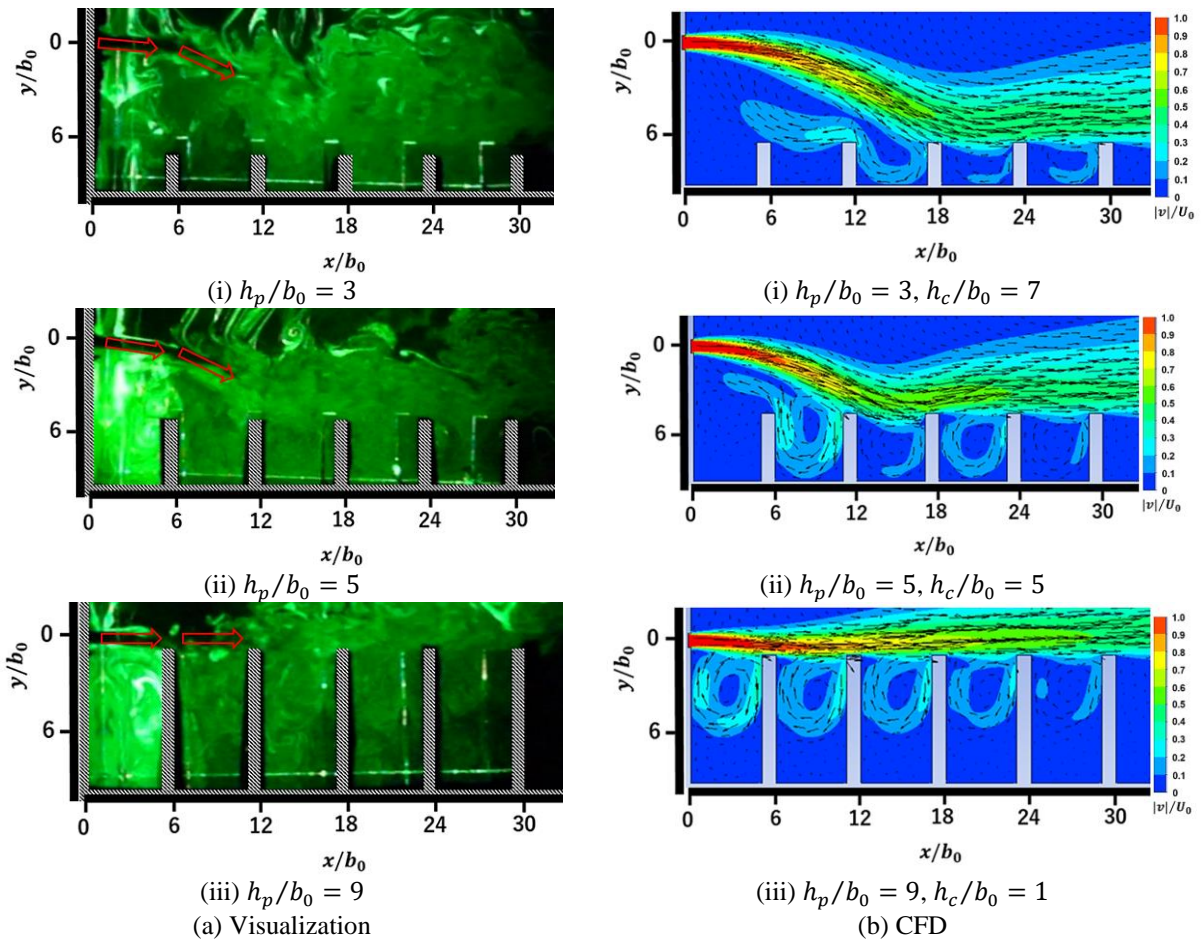


**Fig. 6.** Influence of partition plate length  
( $U_0 = 3.0$  m/s,  $H_s = h_s/b_0 = 10$ ,  $w = 25$  mm,  $b_0 = 5.0 \times 10^{-3}$  m)

Fig. 6 shows the relationship between the flow pattern and the dimensionless partition plate length  $h_p/b_0$  with a constant offset ratio ( $H=10$ ) from the slot to the bottom surface. Similar to the previous figure, the velocity is  $U_0 = 3.0$  m/s, Fig. 6(a) shows the flow visualization photographs, while Fig. 6(b) presents the numerical simulation results. The results for different values of 3, 5, and 9 ( $y_c/b_0 = 7, 5$ , and 1) are presented in (i), (ii), and (iii), respectively. Focusing on the deflection characteristics of the jet flow, the behaviors in Fig. 6 (i), (ii), and (iii) are similar to those in Fig. 5 (iii), (ii), and (i), respectively, suggesting that  $y_c/b_0$  is an important parameter that determines the deflection characteristics. In addition, despite the different cavity sizes in (ii) and (iii), there was slight difference in the size of

the recirculation region. Furthermore, the vorticity inside the cavities in this figure (i), (ii), and (iii) generally corresponds to Fig. 5 (iii), (ii), and (i).

Fig. 7 displays a graph of the inflow rate into each cavity, calculated using CFD. The measurement of inflow rate occurs above the partition plate, with the calculation expressed in Equation (1) below.

$$q_{in} = \frac{1}{2} \int_{x_{s,i}}^{x_{e,i}} |v| dx \quad (1)$$

In graph (a), the outcomes are displayed when  $H_p$  is held constant at 5, while  $H_s$  varies. Conversely, graph (b) demonstrates the results with  $H_s$  maintained at 10 and varying  $H_p$ . An analysis reveals that the condition of  $H_s = 6$  ( $y_c = 1$ ) in Fig. 7(a) closely aligns with that of  $H_p = 9$  ( $y_c = 1$ ) in Fig. 7(b). Furthermore, a parallel can be drawn between the conditions of  $H_s = 10$  ( $y_c = 5$ ) and  $H_p = 5$  ( $y_c = 5$ ) and  $H_s = 14$  ( $y_c = 9$ ) and  $H_p = 3$  ( $y_c = 7$ ). These findings imply that the distance  $y_c$ , measuring from the slot's center to the tip of the partition plate, plays a significant role in influencing the characteristics of the jet flow.

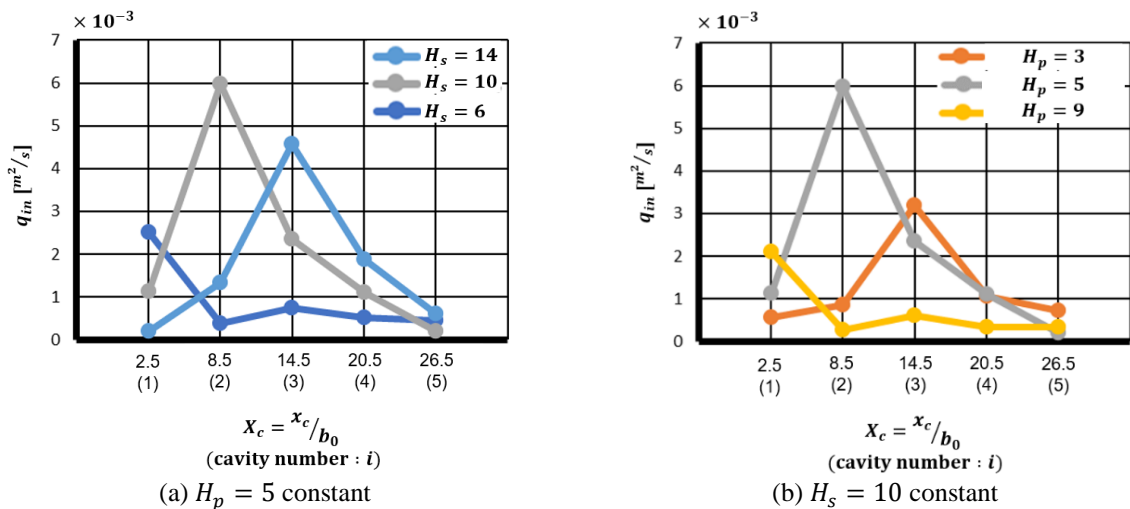


**Fig. 7.** Inflow flow rate into each cavity  
( $U_0 = 3.0 \text{ m/s}$ ,  $w = 25 \text{ mm}$ , and  $b_0 = 5.0 \times 10^{-3} \text{ m}$ )

#### 4. Conclusion

An attempt was made to elucidate the flow characteristics of jet streams passing over seats in passenger compartments such as high-speed trains and airplanes by considering seats as two-dimensional arrays of partition plates. Experiments were conducted using the smoke wire method for flow visualization and numerical simulations were performed. The focus was primarily on the deflection characteristics of the jet streams and size of the recirculation region. In particular, as the distance between the slot outlet height and upper edge of the partition plate decreased, the straightness of the jet streams increased, leading to the formation of recirculation regions with a higher vortex intensity in the flow field.

#### Nomenclature

$b_0$	:	Slot outlet velocity [m/s]
$c$	:	Partition plate width ( $=5 \times 10^{-3}$ [m])
$e$	:	Error rate [%]
$h_p$	:	Partition plate length [m]
$H_p$	:	Dimensionless partition plate length ( $= h_p/b_0$ )
$h_s$	:	Cavity depth from slot center [m]
$H_s$	:	Offset ratio ( $= h_s/b_0$ )

$i$	:	Cavity number
$q_{in}$	:	Cavity inflow flow rate ( $= \int_{x_{s,i}}^{x_{e,i}}  v  dx$ ) [ $m^2/s$ ]
$t$	:	Experimental area height ( $= 1 \times 10^{-1}$ [m])
$u$	:	Velocity [m/s]
$u_e$	:	Experimental velocity [m/s]
$u_t$	:	Numerical analysis velocity [m/s]
$U_0$	:	Slot outlet velocity [m/s]
$v$	:	Vertical velocity [ $m^2/s$ ]
$w_p$	:	Cavity width [m]
$x, y, z$	:	Coordinate axes
$x_c$	:	x-axis cavity center position [m]
$X_c$	:	Dimensionless x-axis cavity center position ( $= x_c/b_0$ )
$y_c$	:	Distance from the bottom of the slot to the tip of the partition plate [m]

## Acknowledgments

This work was supported by JSPS KAKENHI, Grant Number 23K17731, and Hatakeyama Research Grant from the Turbomachinery Society of Japan.

## References

- [1] Park S, Choi Y, Song D, Kim EK. Natural ventilation strategy and related issues to prevent coronavirus disease 2019 (COVID-19) airborne transmission in a school building. *Sci Total Environ.* 2021;789:147764.
- [2] Mason MS, Crowter WJ. Fluidic thrust vectoring of low observable aircraft. CEAS Aerospace Aerodynamic Research Conference; 2002 Jun 10-12; Cambridge, UK. p. 1-7.
- [3] Holman R, Utturkar Y. Formation criterion for synthetic jets. *AIAA J.* 2005;43(10):2110-2116.
- [4] Watabe Y, Sato K, Nishibe K, Yokota K. Influence of an asymmetric slot on the flow characteristics of synthetic jets. In: Segalini A, editor. *Proceedings of the 5<sup>th</sup> International Conference on Jets, Wakes and Separated Flows (ICJWSF2015)*. Cham: Springer; 2016. p. 101-107.
- [5] Kobayashi R, Nishibe K, Watabe Y, Sato K, Yokota K. Vector control of synthetic jets using an asymmetric slot. *J Fluids Eng.* 2018;140(5):051102.
- [6] Kobayashi R, Terakado H, Sato K, Taniguchi J, Nishibe K, Yokota K. Behavior of plane synthetic jets generated by an asymmetric stepped slot. *Int J Fluid Mach Syst.* 2020;13(1):253-265.
- [7] Smith BL, Swift GW. A comparison between synthetic jets and continuous jets. *Exp Fluids.* 2003;34(4):467-472.
- [8] Zhang Q, Takahashi F, Sato K, Tsuru W, Yokota K. Jet direction control using circular cylinder with tangential blowing. *Trans Japan Soc Aero Space Sci.* 2021;64(3):181-188.
- [9] Zhang Q, Tamanoi Y, Kang D, Nishibe K, Yokota K, Sato K. Influence of amplitude of excited secondary flow on the direction of jets. *Trans Japan Soc Aero Space Sci.* 2023;66(2):37-45.